

Electron-energy-loss spectroscopy studies of icosahedral-phase plasmons

L. E. Levine, P. C. Gibbons, and K. F. Kelton

Department of Physics, Washington University, St. Louis, Missouri 63130

(Received 28 June 1989)

Previous electron-energy-loss spectroscopy measurements on amorphous and icosahedral (*i*-phase) Al_6Mn show a broader plasmon excitation in the *i*-phase than in the amorphous phase [Chen *et al.*, *Phys. Rev. Lett.* **57**, 743 (1986)]. This broadening is presumed to arise from differences between the electronic structures of the phases. We present measurements on *i*-phase Al_6Mn that confirm these earlier results. We also present measurements that show plasmon widths that are similar in *i*-phase and amorphous $\text{Pd}_{58.8}\text{U}_{20.6}\text{Si}_{20.6}$, and in *i*-phase and amorphous $\text{Al}_{75}\text{Cu}_{15}\text{V}_{10}$. Thus, the additional broadening in *i*-phase Al_6Mn is not a general feature of the icosahedral phase. The phase independence of plasmon widths in $\text{Pd}_{58.8}\text{U}_{20.6}\text{Si}_{20.6}$ and $\text{Al}_{75}\text{Cu}_{15}\text{V}_{10}$ suggests that the amorphous and icosahedral phases in these systems have similar short-range ordering.

INTRODUCTION

Possible structural similarities between icosahedral phases (*i*-phase) and amorphous phases are interesting because of their relevance to formability, metastability, and structure of the *i*-phase. While many probes can be used to examine short-range ordering (SRO) in bulk materials (nuclear-magnetic resonance, Mössbauer, extended x-ray-absorption fine-structure spectroscopy, etc.), electron-energy-loss spectroscopy (EELS) has the additional advantage of allowing measurements on individual microscopic grains. This enables studies of the majority of *i*-phase alloys that have grains smaller than 10 μm .

Several EELS studies of *i*-phase alloys have been reported.¹⁻⁵ Most of these used bulk-plasmon measurements to determine optical conductivities in *i*-phase Al_6Mn , *i*-phase AlLiCu , and related crystal phases.²⁻⁴ Bahadur, Gaskell, and Imeson looked at the Mn L_3/L_2 ratio in an attempt to examine the local coordination of Mn in *i*-phase Al_6Mn .⁵ Finally, Chen *et al.* observed a significant broadening of the bulk plasmon in *i*-phase Al_6Mn over amorphous and crystalline Al_6Mn .¹ In contrast to these earlier studies, we have concentrated on the relationship between icosahedral and amorphous phases in different alloys. As a result, we can for the first time identify two classes of materials, those with similar SRO in their amorphous and *i*-phases, and those with measurably different SRO's.

Plasmons are long wavelength, collective, electronic excitations in solids. The energy width of the plasma resonance is determined by the damping in the system; the primary source of plasmon damping is single-electron excitations (vertical interband transitions in crystals).⁶ Therefore, any difference between the plasmon widths in *i*-phases and amorphous phases of identical composition must be due to differences between the spectra of single-electron excitations in the energy range from 5–30 eV. There must be corresponding differences between the complex dielectric functions of the phases.

EELS measurements by Chen *et al.*¹ on amorphous, *i*-phase, and orthorhombic Al_6Mn gave plasmon energy

widths [full width at half maximum (FWHM)] of 2.4, 3.1, and 2.2 eV, respectively. Since the plasmon widths were similar in the amorphous and crystalline phases, they concluded that the broadening of the *i*-phase Al_6Mn plasmon is not due to increased lattice disorder, but arises from a different electronic structure of the *i*-phase.

Chen *et al.* hypothesized that the presence of an incommensurate lattice spacing should allow many new channels for interband transitions. If true, this should broaden the plasmons of all icosahedral phases. We confirm Chen's plasmon results for *i*-phase Al_6Mn but have found two other systems that have no more plasmon broadening in their *i*-phases than in their amorphous phases: $\text{Al}_{75}\text{Cu}_{15}\text{V}_{10}$ and $\text{Pd}_{58.8}\text{U}_{20.6}\text{Si}_{20.6}$.

SAMPLE PREPARATION

Alloys of the appropriate composition were produced by induction melting in fused silica crucibles in 0.5 atm of Ar. These samples were broken up and melt spun onto a rapidly rotating copper wheel in 0.5 atm Ar to produce ribbons that were 20–30 μm thick by 2–4 mm wide. The Al_6Mn sample was quenched directly into the *i*-phase. The $\text{Pd}_{58.8}\text{U}_{20.6}\text{Si}_{20.6}$ and $\text{Al}_{75}\text{Cu}_{15}\text{V}_{10}$ alloys were quenched to amorphous phases and transformed to *i*-phases by annealing. As described by Tsai, Inoue, and Masumoto⁷ a wheel speed of ≈ 55 m/sec was necessary to obtain amorphous $\text{Al}_{75}\text{Cu}_{15}\text{V}_{10}$. The wheel speed was less critical in the other two systems. All samples for transmission-electron-microscopy (TEM) studies were thinned in a liquid-nitrogen cooled ion mill using low beam currents to minimize damage.

Amorphous $\text{Pd}_{58.8}\text{U}_{20.6}\text{Si}_{20.6}$ was transformed by annealing in vacuum at 490 °C for 110 min. TEM studies showed that the transformed sample was approximately 70% *i*-phase and 30% amorphous phase. The *i*-phase occurred as roughly spherical nodules ranging from 100–1000 Å diam embedded in the amorphous phase.

The amorphous $\text{Al}_{75}\text{Cu}_{15}\text{V}_{10}$ was transformed in a nitrogen-purged differential scanning calorimeter (DSC).

The sample was heated to 500 °C at a rate of 20° per min. TEM studies showed that the sample was approximately 60% *i*-phase. The remainder was a fine dispersion of microquasicrystalline grains embedded in an amorphous matrix. The cross sections of the large icosahedral grains were roughly circular and ranged up to 4000 Å in diameter.

Selected area electron diffraction (SAD) patterns from *i*-phase Al₇₅Cu₁₅V₁₀ showed two unusual features. First, the twofold and $[\bar{1}10]$ orientations exhibited diffraction spots at the extinct odd-parity locations. Indexing demonstrates that the Al₇₅Cu₁₅V₁₀ *i*-phase has diffraction patterns corresponding to a six-dimensional body-centered cubic reciprocal lattice. In addition, the SAD patterns contain intense arcs of diffuse scattering which appear to be identical to those found in *i*-phase TiMn.⁸ Both of these features will be discussed in a future publication.

EELS MEASUREMENTS

Measurements were made using a Gatan model 607 EELS attached to a JEOL 2000FX TEM, at 120-keV beam energy. Diffraction measurements have previously been published for all the amorphous and icosahedral phases examined in this study.^{7,9,10} We confirmed these results by SAD from all grains used to obtain EELS data. Energy dispersive x-ray spectroscopy (EDS) measurements established that there was no stoichiometric difference between the amorphous phase and the *i*-phase in Pd_{58.8}U_{20.6}Si_{20.6} and Al₇₅Cu₁₅V₁₀.

EELS measurements were made on sample regions of nearly uniform thickness. In the worst case, the double-scattering feature at twice the plasmon energy had an area of ≈ 25% (typically under 10%) of the plasmon area. In all cases, the peaks were well separated demonstrating that multiple-scattering effects on the plasmons were negligible.

When possible, EELS spectra were taken from individual grains that were rotated to low-symmetry orientations to minimize effects of coherent elastic scattering. A momentum transfer acceptance of 3.2 Å⁻¹ diam, centered on the forward scattering direction, was used to obtain adequate count rates. The effect of energy dispersion on the plasmon widths was negligible for this acceptance value [see Fig. 1(a)].

EELS measurements of Al₆Mn were made on the *i*-phase only. All measurements were made on an individual grain with a diameter of ≈ 1 μm so that finite-size effects remained small. A typical plasmon spectrum from *i*-phase Al₆Mn is shown in Fig. 1(b). The results from 26 energy loss scans were averaged to give the plasmon-width results reported in Table I. A direct comparison with the results of Chen *et al.* is not possible due to our different instrumental resolutions. Correcting our data for the measured instrumental resolution (1.19 ± 0.02 eV FWHM) yields a width of 3.17 ± 0.02 eV, which compares favorably with Chen's corrected value of 3.09 eV.

The small size of the Pd_{58.8}U_{20.6}Si_{20.6} *i*-phase grains (≤ 1000-Å diam) made EELS measurements on a single grain impossible. The largest diameter was comparable to the plasmon wavelength which resulted in interference

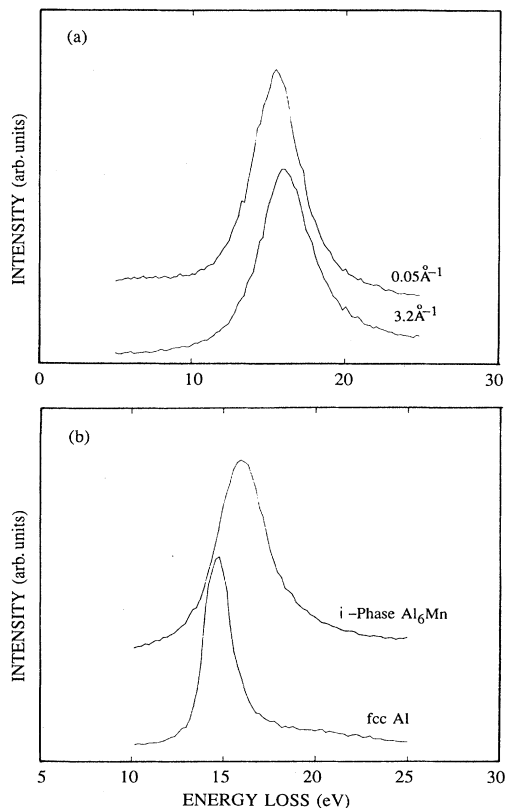


FIG. 1. (a) EELS plasmon spectra of amorphous Al₇₅Cu₁₅V₁₀ collected using momentum transfer acceptances of 3.2 and 0.05-Å⁻¹ diam. A small peak shift is evident, but the width is constant. (b) EELS plasmon spectra of *i*-phase Al₆Mn and polycrystalline Al. Averaged characteristics are shown in Table I. There is an arbitrary offset between the curves.

with the grain boundaries and made any measurements unreliable. To overcome this difficulty, we collected data from a region ≈ 20 μm in diameter, thus averaging over the amorphous phase and ≈ 400 *i*-phase grains. EELS measurements were also made on the as-quenched amorphous material. Since the *i*-phase grains in the annealed sample are roughly spherical and are small compared with the plasmon wavelength, dynamic effective medium theory¹¹ (DEMT) may be used to separate out the complex dielectric function¹² of the *i*-phase component.

Figure 2(a) shows typical spectra obtained from a mixture of amorphous and *i*-phase, and from single-phase amorphous Pd_{58.8}U_{20.6}Si_{20.6}. Since all spectra were taken

TABLE I. The *i*-phase Al₆Mn and polycrystalline Al plasmons.

Phase	FWHM (eV)	Mean (eV)
Al ₆ Mn	3.39 ± 0.02	15.68 ± 0.08
fcc Al	1.84 ± 0.05	14.74 ± 0.04
Resolution-corrected FWHM		
Present work (eV)	3.17 ± 0.02	
From Ref. 1 (eV)	3.09	

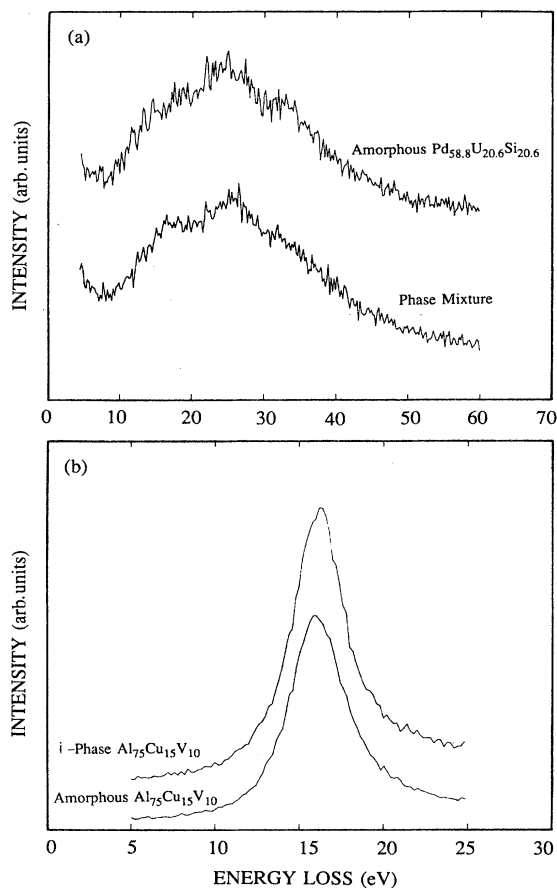


FIG. 2. (a) EELS plasmon spectra from amorphous Pd_{58.8}U_{20.6}Si_{20.6} and from a phase mixture of 30% amorphous and 70% *i*-phase Pd_{58.8}U_{20.6}Si_{20.6}. Averaged characteristics are shown in Table II. (b) EELS plasmon spectra of *i*-phase and amorphous Al₇₅Cu₁₅V₁₀. Averaged characteristics are shown in Table III. There is an arbitrary offset between the curves.

under identical conditions, no instrumental resolution corrections were made on this data. The spectra are complex (multicomponent) because U has many one-electron excitations in the energy range where the plasmons appear. Averaging over nine scans gives a plasmon width of 34.70 ± 0.32 eV for the amorphous material; ten scans give 34.40 ± 0.26 eV for the phase mixture (see Table II). This difference of one standard deviation is not significant. A DMT analysis of these results confirmed that the plasmon width of the *i*-phase was indistinguishable from

TABLE II. Pd_{58.8}U_{20.6}Si_{20.6} plasmons.

Phase	FWHM (eV)	Mean (eV)
Amorphous	34.70 ± 0.32	24.82 ± 0.13
Mixture	34.40 ± 0.26	24.52 ± 0.24
Differences (amorphous - mixture)		
FWHM (eV)	0.30 ± 0.26	
Mean (eV)	0.30 ± 0.41	

TABLE III. Al₇₅Cu₁₅V₁₀ plasmons.

Phase	FWHM (eV)	Mean (eV)
Amorphous	4.11 ± 0.04	15.96 ± 0.05
<i>i</i> -phase	3.93 ± 0.07	16.34 ± 0.05
fcc aluminum	1.84 ± 0.05	14.74 ± 0.04
Differences (amorphous - <i>i</i> -phase)		
FWHM (eV)	0.18 ± 0.08	
Mean (eV)	-0.38 ± 0.07	

that of the amorphous phase.

EELS measurements of amorphous and *i*-phase Al₇₅Cu₁₅V₁₀ were more reliable. Large *i*-phase grains of uniform thickness were plentiful and the plasmon structures of the phases examined were narrow and single component. Typical spectra from *i*-phase and amorphous Al₇₅Cu₁₅V₁₀ are shown in Fig. 2(b); the results are tabulated in Table III. As with the Pd_{58.8}U_{20.6}Si_{20.6}, no instrumental resolution corrections were made on this data. Averaging over nine scans gives a plasmon width of 3.93 ± 0.07 eV for the *i*-phase; nine scans give 4.11 ± 0.04 eV for the amorphous phase. Subtracting these values results in a width difference of 0.18 ± 0.08 eV. Because small changes in the tuning of the EELS or the TEM between measurements might produce such a difference, it cannot be considered significant.

CONCLUSION

We have determined that the large plasmon-width increase reported between amorphous and *i*-phase Al₆Mn does not occur in Pd_{58.8}U_{20.6}Si_{20.6} or Al₇₅Cu₁₅V₁₀. This result disproves the hypothesis of Chen *et al.* that the width increase was caused by the presence of an incommensurate lattice spacing that should allow many new channels for interband transitions.¹ Their hypothesis is invalid since factors other than the high density of reciprocal-lattice vectors are involved. The damping of a long-wavelength plasmon by a vertical interband transition depends on the oscillator strength of that transition, and therefore on the Fourier component of the quasilattice potential at the reciprocal vector, *g*, associated with it.¹³ Although the reciprocal quasilattice is dense with *g* vectors, only a few have sufficiently large potential components to contribute significantly to plasmon damping.

Since the screening lengths in these metal alloys are no more than a few Å, any differences in electronic structure are caused by differences in local clusters. In this work, elemental differences have been eliminated leaving structural changes as the most likely explanation. Therefore, we conclude that the SRO in *i*-phase Al₆Mn differs from the SRO in the amorphous phase. No such change in the SRO was detected in the plasmon measurements of Pd_{58.8}U_{20.6}Si_{20.6} and Al₇₅Cu₁₅V₁₀. We suggest that the difference in preparation of amorphous Al₆Mn (sputtering), and *i*-phase Al₆Mn (rapid quenching) may be responsible for the differences in SRO observed by Chen *et al.*

ACKNOWLEDGMENTS

We thank Joe Holzer for his assistance in sample preparation. This research was partially supported by National Science Foundation Grant No. DMR-86-04148.

-
- ¹C. H. Chen, D. C. Joy, H. S. Chen, and J. J. Hauser, *Phys. Rev. Lett.* **57**, 743 (1986).
²J. L. Verger-Gaugry, P. Guyot, and M. Audier, *Phys. Lett. A* **117**, 307 (1986).
³J. L. Verger-Gaugry and P. Guyot, *J. Phys. (Paris) Colloq.* **47**, C3-477 (1986).
⁴P. Sainfort and P. Guyot, *Scr. Metall.* **21**, 1517 (1987).
⁵D. Bahadur, P. H. Gaskell, and D. Imeson, *Phys. Lett. A* **120**, 417 (1986).
⁶P. C. Gibbons, *Phys. Rev. B* **23**, 2536 (1980), and references therein.
⁷A. P. Tsai, A. Inoue, and T. Masumoto, *Jpn. J. Appl. Phys.* **26**, L1994 (1987).
⁸P. C. Gibbons, K. F. Kelton, L. E. Levine, and R. B. Phillips, *Philos. Mag. B* **59**, 593 (1989).
⁹S. J. Poon, A. J. Drehman, and K. R. Lawless, *Phys. Rev. Lett.* **55**, 2324 (1985).
¹⁰D. Sheckman, I. A. Blech, D. Gratias, and J. W. Cahn, *Phys. Rev. Lett.* **53**, 1951 (1984).
¹¹D. Stroud and F. P. Pan, *Phys. Rev. B* **17**, 1602 (1977).
¹²S. E. Schnatterly, *Solid State Physics*, edited by H. Ehrenreich, F. Seitz, and D. Turnbull (Academic, New York, 1979), Vol. 34, p. 285.
¹³P. C. Gibbons and S. E. Schnatterly, *Phys. Rev. B* **15**, 2420 (1976).